Research Journal of
Applied Science
MEDWELL PUBLICATIONS

Comparative Study Between Controllers for Tracking Systems in a Microgrid

Mauricio F. Mauledoux M., Oscar F. Avilés S., Edilberto Mejía R., Oscar I. Caldas F. and Angie J. Valencia
Mechatronics Engineering Program, Faculty of Engineering, Militar Nueva Granada University, Bogota, Colombia

Key words: DC microgrids, fuzzy control, MIT rule, PV module, renewable energies, solar irradiance, servo control system

Corresponding Author:
Mauricio F. Mauledoux M.
Mechatronics Engineering Program, Faculty of Engineering, Militar Nueva Granada University, Bogota, Colombia

Page No.: 380-387
Volume: 14, Issue 11, 2019
ISSN: 1815-932x
Research Journal of Applied Sciences

Abstract: The implementation of renewable energy systems is a growing activity, due to lack of nature reserves, the pollution excess and the continuous demand in the use of energy supply for the common life needs. This means that people must change the way they use the environmental resources to get it, using green energy as that provided by wind or solar sources. Therefore, this work shows the results obtained after performing a comparative analysis between the static behaviors and those achieved using the following controllers in a single axis solar Photovoltaic (PV) tracking system: fuzzy, servo system and MIT rule-based. The PV modules position were defined according to the maximum solar irradiance, when the sun reaches its zenith (90°). The data used in the controllers design and simulation were collected during a meteorological study made with the weather station of the regional environmental authority (CAR), located in Militar Nueva Granada University's Campus at Cajica, Colombia.

INTRODUCTION

Nowadays, the demand for energy and the associated services is increasing which influences the economic development and the human health as requirements to supply the basic needs as cook, lighting, mobility and communication. Since 1850, the global energy has been generated using fossil fuels such as coal, oil and gas, leading to a rapid growth in carbon dioxide emissions (Edenhofer *et al*., 2011). In addition, the Greenhouse Gas (GHG) has contributed significantly to increase atmospheric GHG concentrations according to the intergovernmental panel on climate change in its fourth Assessment Report (AR4).

On a global basis, it is estimated a growth in the global power capacity to exceed 1,560 GW at the end of 2014, up >8% over 2012. The hydropower capacity grew 4% to about 1,000 GW and other renewables collectively (wind, solar, geothermal, biomass and biofuels) nearly 17% to >560 GW (REN 21, 2014); besides, the world added more solar energy than wind power capacity for the first time, solar Photovoltaic (PV) and hydropower reached together about one-third of new capacity and the first one has grown almost 55% annually over the past 5 years. In 2013, renewables accounted for >56% of global power capacity and represented higher additions in several countries.

There are multiple solutions for lowering the emissions from the energy system that will still satisfy the global demand for human services. One of these is the mentioned renewable energy which is evaluated to get its contribution to sustainable development and all associated risks and costs. All this, there is an interest of how meteorological condition play a significant role in the

performance of renewable systems whereas these systems produce optimum output under certain desired weather conditions mainly related with its location (Uchida, 2009). To use renewable energy systems, it is necessary to perform smart microgrids that allow the integration of a remarkable amount of bioenergy suppliers, such as solar, geothermal, hydropower, ocean and wind energy, improving reliability, quality of supply and ensuring safety; due to the great advantages, it is necessary to analyze how energy should be used in those microgrids (Shah *et al*., 2012).

The microgrids are components in a distribution network that can be supplied and operated independently (Dobakhshari *et al*., 2012). In addition, it is a hybrid system consisting of a set of conventional renewable energy operating as a process able to provide continuous energy in the electricity supply (Fossati, 2011). The current tendency is to project this kind of systems with green sources providing 80-90% of the energy needed in remote or non-electrified areas. In order to implement it, the use of solar energy as a renewable energy system is taken into account, making necessary to apply a PV or concentrating solar power to produce energy through sunlight and its maximum irradiance.

The implementation of the PV collection system becomes complete when it uses a mechanism that allows solar tracking by means of photosensitive resistances and stepper motors, considering the option to be switched off at night or cloudy days (Liu *et al*., 2011). In addition, it is necessary to consider a design based on the respond to environmental behaviors using parameters as real-time responsiveness, reliability, stability and safety. Definitely, it is essential to design a mechatronic system stable and robust enough to be resistant to fluctuating weather conditions and minor mechanical stresses (Juang and Radharamanan, 2014). Also, this work shows the mathematical PV model (also called solar panel), besides the implementation and simulation of the fuzzy, servo-system and adaptive angular position control systems. The system determined the ideal position based in the maximum irradiance measured by a pyrometer. Finally, as a main contribution, this study presents the results of the comparison of the proposed control systems efficiency in a static reference point.

Mathematical tracking model: The mathematical model of the complete system was divided in two parts: the first one was the PV module model and the other one was mechanical system which was represented by the DC motor model. The photovoltaic module is represented as two electrical circuit nodes with the sunlight as current source (photocurrent), along with a diode connected in anti-parallel and both series and parallel resistances, as shown in Fig. 1.

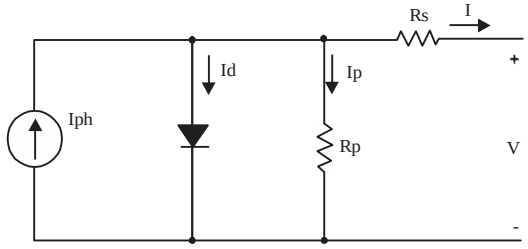

Fig. 1: Simplified model of photovoltaic module

This is a non-linear system that include parameters that can be classified in three groups: manufacturing data, electrochemical constants that can be use considering the environmental and those that can be calculated. The aim of this work is to obtain a model representation as close as possible to the experimental measures but trying to make it easy to computer calculations, thus, it has the possibility to operate with few parameters but still working similarly in order to obtain a valid approximation. Therefore, none of the parameters were simplified or ignored.

According to the model depicted in Fig. 1, the equation that defines the photovoltaic model dynamics in terms of an output current by the Kirchhoff's current law, is shown in Eq. 1:

$$I = I_{ph} - I_d - I_p \tag{1}$$

The ohm's law let to define the current through the parallel resistance Eq. 2. The photocurrent is a relative value of the reference and variations produced by the cells temperature Eq. 3:

$$I_p = \frac{V+R_sI}{R_p} \tag{2}$$

$$I_{ph} = \frac{G}{G_{ref}}\left(I_{ph,ref} + \mu_{sc}\Delta T\right) \tag{3}$$

Where:

V = The diode voltage is the solar irradiance
G = The solar irradiance at Standard Test Conditions (STD)
ΔT = The PV cells temperature variation
μ_{sc} = The temperature coefficient of short circuit current

The diode current is given by the Shockley Eq. 4:

$$I_d = I_o\left[\exp\left(\frac{V+IR_s}{a}\right)\right] \mid a = AN_sV_T \tag{4}$$

Where:

A = The ideal factor for monocrystalline silicon cells
N_s = The number of PV cells connected in series
V_T = The thermal factor defined in Eq. 5
I_o = The reverse saturation or leakage current Eq. 6

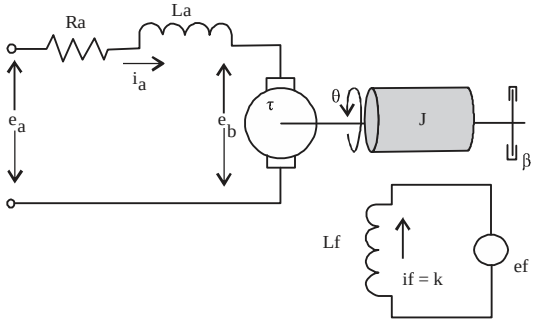

Fig. 2: Motor DC representation

Table 1: PV module parameters

Bosch c-Si M60-M260		STC constants	
Parameters	Values	Parameters	Values
N_s	60	k	$1{,}381.10^{-23}$
P_{mp}	260	q	$1{,}602.10^{-19}$
V_{mp}	30,71	G_{ref}	1000
I_{mp}	8,47	$T_{c,\,ref}$	298
I_{sc}	9,02	-----Variables to be obtained-----	
V_{oc}	38,1	R_s	R_p
π_{sc}	3,1	I_{ph}	I_o
A	1,2	----------Inputs----------	
ε_G	1,12	G	T_c

$$V_T = k\frac{T_C}{q} \tag{5}$$

Where:

k = The Boltzmann constant
q = The electron charge
T_c = The current cell temperature

$$I_o = I_{o,\,ref}\left(\frac{T_c}{T_{c,\,ref}}\right)^3 \exp\left[\left(\frac{q\varepsilon G}{Ak}\right)\left(\frac{1}{T_{c,ref}}-\frac{1}{T_c}\right)\right] \tag{6}$$

Equation 6 depends on the electrochemical constants, including the material band gap energy ε_G as well as the temperature and the reference leakage current on diode $I_{o,\,ref}$, defined in Eq. 7 in terms of the voltage at open circuit and the STC conditions:

$$I_{o,\,ref} = I_{sc}\exp\left(\frac{-V_{oc,\,ref}}{a}\right) \tag{7}$$

The photovoltaic parameters to define the model with the equations shown above are given in Table 1, corresponding to a Bosch c-Si M60-M260 photovoltaic cell.

The model second part (mechanical system) consists in a motor that allows the PV module to move in order to reach the maximum energy using the solar irradiance, depending on the tracking structure position and the sunlight parameters. To get the ideal mathematical representation, it is necessary to use the diagram shown in Fig. 2.

To obtain the mathematic model of the motor, it is necessary to consider both electrical and mechanical parts system. In this case the electrical part is given by Kirchhoff's Law Eq. 8 and the mechanical is represented by Eq. 9 (Shah *et al*., 2012; Sastry and Bodson, 1989; Anonymous, 2014a, b):

$$v_a(t) = R_a i_a(t) + L_a\frac{di_a(t)}{dt} + e_a(t) \tag{8}$$

$$T(t) = J\frac{d\omega(t)}{dt} + B\omega(t) \tag{9}$$

Equation 8 and 9 are linked by the relationship given in Eq. 10 and Eq. 11:

$$T(t) - T_L = K_m i_a(t) \Rightarrow T_L = 0 \tag{10}$$

$$e_a(t) = K_e\omega(t) \tag{11}$$

Equation 11 defines the voltage of Electromagnetic Field (EMF) which is replaced in Eq. 8 to obtain the armature voltage Eq. 12, then. The same procedure is made with Eq. 9 and 10 to get the armature current Eq. 13 and so, the entire DC motor representation Eq. 14:

$$v_a(t) = R_a i_a(t) + L_a\frac{di_a(t)}{dt} + K_e\omega(t) \tag{12}$$

$$i_a(t) = \frac{J}{K_m}\frac{d\omega(t)}{dt} + \frac{B}{K_m}\omega(t) \tag{13}$$

$$v_a(t) = \frac{R_a J}{K_m}\frac{d\omega(t)}{dt} + \frac{R_a B}{K_m}\omega(t) + \frac{L_a J}{K_m}\frac{d^2\omega(t)}{dt} + \frac{L_a B}{K_m}\frac{d\omega(t)}{dt} + K_e\omega(t) \tag{14}$$

To simulate the process, the parameters of the tracking system motor are obtained. In this case, an standard motor is used to make the simulations, considering: $R_a = 4\Omega$, $L_a = 2{,}750\times10^{-6}$ H, B = 30228 Nm. s/rad, ke = 0,027 Vs/rad, Km = 0,027 Nm/A and J = $3{,}3228\times10^{-6}$ kg.m^2.

Finally, the space state representation is obtained using the system matrix Eq. 15, the input matrix Eq. 16, the output matrix Eq. 17 and the hitch matrix Eq. 18:

$$A = \begin{bmatrix} \frac{-R_a}{L_a} & \frac{-K}{L_a} \\ \frac{K}{J} & \frac{-B}{J} \end{bmatrix} = \begin{bmatrix} -400 & -2.74 \\ 8487{,}2 & -1{,}0865 \end{bmatrix} \tag{15}$$

$$B = \begin{bmatrix} \frac{1}{L_a} \\ 0 \end{bmatrix} = \begin{bmatrix} 100 \\ 0 \end{bmatrix} \tag{16}$$

$$C = [0 \quad 1] \tag{17}$$

$$D = [0] \tag{18}$$

MATERIALS AND METHODS

Control models implemented

Fuzzy logic control: The fuzzy logic is presented as a very useful strategy in the control systems development using a knowledge base that allows the designer to define rules considering the system behavior. Also, it handles non-exact information and sometimes qualitative values called as linguistic values (Vidal, 2014).

The fuzzy controller needs to previously define the system input and output variables. The output signal (angular position) is limited to a maximum rotation of 10° which assures a soft and constant movement to the PV module to arrive to desire points in an appropriate way (Mauledoux *et al*., 2016). Meanwhile, the input is defined as the difference between the structure current angle and the desire one to reach maximum irradiance.

Once the variables to handle (controller input and output) are clearly defined, the design process continues with the fuzzy sets creation. Figure 3 shows how the input signal is classified through five fuzzy sets; four of them are trapezoidal and one triangular, arranged in such a manner that cover all values from -90°- 90°. This range was defined according to a study case that concluded a variation between 45° and 135°.

Regarding to the controlled variable (output), Fig. 4 shows five sets, four of them are trapezoidal and the last one is triangular, proportionally distributed from -10° to 10°. Therefore, when de angular position error (input) is positive, the controller respond with an increase in the output value, producing a rise in the system position but if the system error is negative then that output controller has to decrease until the PV module arrives to the right position and maximize power.

When we defined the structure of fuzzy sets, we proceed with the rules that define the relationship between the error and control signals, i.e., if the error is negative then the controller has to handle a signal decrement until the system error gets to zero and the opposite if it would have been positive (increment). A low proportion of this two let to define the leftover rules and then complete the process. The design finalizes with the sets inferences by means of the input or output degree of membership in the final fuzzy sets; then, a defuzzification process is made with the centroid method as shown in Eq. 19:

$$y_{centroid} = \frac{\sum_{x \in X} x\mu_A(x)}{\sum_{x \in X} \mu_A(x)} \tag{19}$$

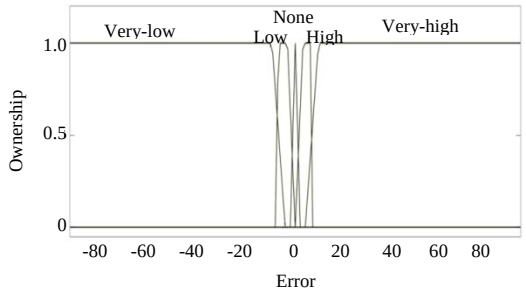

Fig. 3: Graphics of Input fuzzy sets

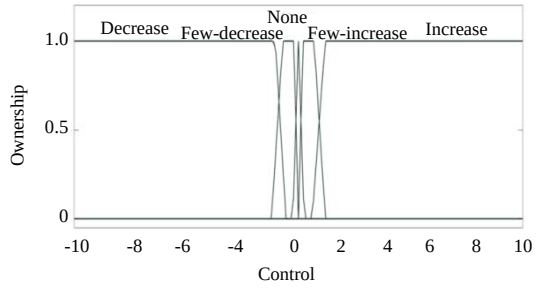

Fig. 4: Graphics of Output fuzzy sets

Servo-system control: In the servo-system it is necessary to take into account the controllability and observability matrices, due to the fact that some important properties of the state-space models must be studied prior to the controller design.

Controllability deals with the possibility of forcing the system to a particular state according to the control input; if a state is uncontrollable then no input will be able to be controllable. On the other hand, whether or not the initial states can be observed from the output is determined using the observability property, so, if a state is not observable then the controller will not be able to determine its behavior from the system output and hence, not be able to use that state to stabilize the system (Indrani-Kar and Majhi, 2015). Figure 5 shows a representation of the servo-system controller.

The continuous-time controllability matrix is given by Eq. 20 and the observability matrix is shown in Eq. 21. Both matrices consider the state-space matrices A, B and C:

$$Mc = [B \; AB, \cdots, A^{n-1}B] \tag{20}$$

$$Mo = \begin{bmatrix} C \\ CA \\ \vdots \\ CA^{n-1} \end{bmatrix} \tag{21}$$

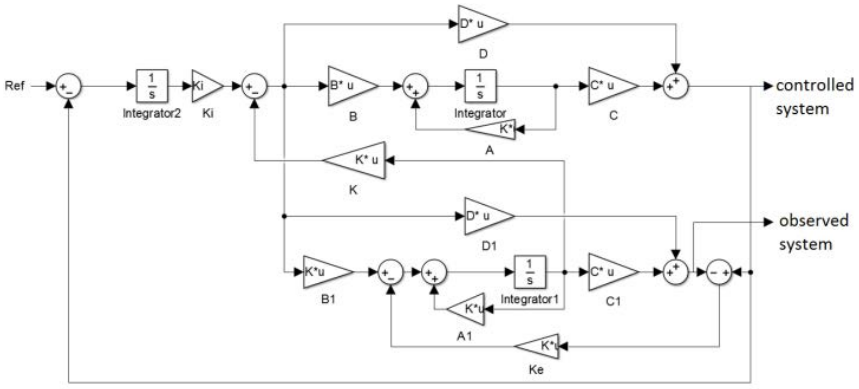

Fig. 5: Servo-system representation

To obtain the coefficients of the control law, the Ackermann method has to be implemented adding an integral action to stabilize it in the desire reference (remove the steady-state error). This additional integrator state augment the matrices to the shown in Eq. 22 and 23:

$$Ae = \begin{bmatrix} A & 0 \\ -C & 0 \end{bmatrix} \quad (22)$$

$$Be = \begin{bmatrix} B \\ 0 \end{bmatrix} \quad (23)$$

Ackermann method: To develop the Ackermann method is required to use some parameters of the first controller, such as the damping coefficient ξ and the undamped natural frequency to get the desire response. This allows the designer to calculate the desired response polynomial as shown in Eq. 24:

$$P_d = s^2 + 2\omega n\xi s + \omega n^2 \quad (24)$$

After, all s variables are replaced with the A matrix and the s^0 by the identity matrix getting $\varphi(A)$ as shown in Eq. 25 (Ackermann and Utkin, 1998):

$$\varphi(A) = A^2 + a_1 A + a_0 I \quad (25)$$

The controller coefficients are obtained by Eq. 26, using the matrix equations Eq. 20 and 25:

$$K = [00, \ldots, 01]\text{inv}(Mc)\varphi(A) = [-3{,}9982 - 0{,}02733{,}1645 \cdot 10^{-4}] \quad (26)$$

Finally, the observability system is calculated taking into account none overshot which implies a damping coefficient $\xi = 1$ and thus, a system without oscillation. Furthermore, the observer need to have a settling time 10 times faster than the close loop system, so, the Ackermann method has to be performed once again with these new parameters to obtain the observer coefficients, as shown in Eq. 27:

$$Ke = \begin{bmatrix} 0 \\ 0 \\ \vdots \\ 0 \\ 1 \end{bmatrix} \text{inv}(Mo)\varphi(A) = [2{,}4925 \cdot 10^8 - 0{,}0145 \cdot 10^8] \quad (27)$$

Adaptive control using MIT rules: The main idea of this controller is to create a closed loop with parameters that can be modified to change the system response and thus, get a behavior similar to the desired model. When the controller is implemented, the designer chooses the reference model, the control structure and the tuning gains for the mechanism adjustment.

Before designing an adaptive controller it is necessary to know how a MIT rule has to be applied. In this case, the control begins with defining the error; it is the difference between the system (y_p) and the reference model (y_m) outputs as shown in Eq. 28:

$$e = y_p - y_m \quad (28)$$

Then it is required to define the cost function $J(\theta)$. The choice of this function can be made considering the adjustment parameters, so, in Eq. 29 this function is displayed:

$$J(\theta) = \frac{1}{2}e^2(\theta) \quad (29)$$

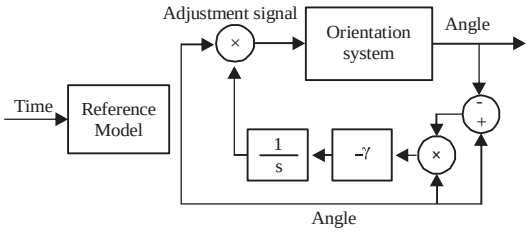

Fig. 6: Adaptive control diagram

The parameter that can be found defining the aim of this calculation which in this case is to minimize the cost in the error which is sensible to move in negative direction of the J's gradient. In order to implement it, the θ time derivative that is known as MIT rule is shown in Eq. 30:

$$\frac{d\theta}{dt} = -\gamma\frac{\delta J}{\delta\theta} = -\gamma e\frac{\delta e}{\delta\theta} \tag{30}$$

where, γ is the adaptive gain. For this control technique it is important to use the gradient, it means that Eq. 30 have to be modified until it get the representation shown in Eq. 31 (Landau, 1974; Shankar, 1994):

$$\Delta\theta^*(e,t) = -\gamma\text{grad}(J) = -\gamma\frac{\partial J}{\partial\theta} \tag{31}$$

where, Δθ* is the variation of θ* regarding to the last value of γ. Then, the adjustable parameter regarding to time is shown in Eq. 32. Finally, the MIT rule is applied to give an expression for θ updating (33):

$$\theta^* = -\gamma\frac{\partial}{\partial t}\left(\frac{\partial J}{\partial\theta}\right) = -\gamma\frac{\partial}{\partial\theta}\left(\frac{\partial J}{\partial t}\right) = -\gamma\frac{\partial}{\partial\theta}\left(\frac{1}{2}e^2\right) \tag{32}$$

$$\theta^* = -\gamma\, e\, y_m \tag{33}$$

The block diagram for this control is shown in Fig. 6. It is important to note that the MIT rule by itself does not guarantee convergence or stability.

Control implementation in the photovoltaic system: To apply the control strategies it is necessary to follow the scheme shown in Fig. 7 which allows to easily understand the implementation of the adaptive control in a tracking system and the relationship between it and the PV system.

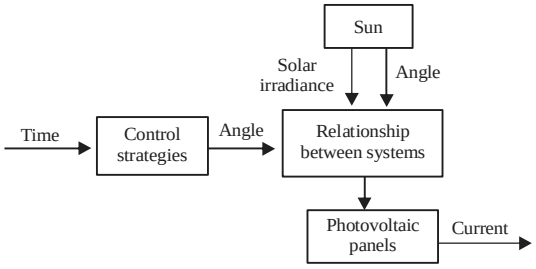

Fig. 7: Interconnection between control and photovoltaic system

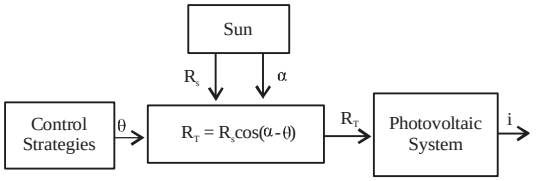

Fig. 8: Relationship between control strategies and solar panel model

The relationship between the tracking system and the PV module dynamics to get the final current is shown in Fig. 8. Where θ is the angle given by the orientation system, R_s is solar irradiance, α is the angle of solar position, R_T is the irradiance at which the module needs to work and is the current produced by the PV system. It is observed that R_T is directly influenced by the difference between the angle given by the controllers and the other set by the solar irradiance. The control has to guarantee an error signal around zero that means a maximum concentration of solar energy.

RESULTS AND DISCUSSION

The simulation result shows that the tracking controllers always tends to follow the maximum theoretical transfer of irradiance to the PV module that occurs when the position of the sun and the PV panel are perpendicular (90°). Figure 9 and 10 shows max current that can be obtained, static position of structure at the usual 5° of orientation, MIT adaptive control, servo-system control and the fuzzy controller where the total current generated with the static position of structure correspond to 82.13% and the solar tracking with a fuzzy controller obtained a 98.26%, MIT adaptive control obtained a 97.96% and servo-system control obtained a 98,38% of the maximum current that can be obtained. The test was made with randomly selected day of the data obtained by the weather station. These results are shown in Fig. 11 with a comparative bar chart of total current obtained in the tests that represent one day or 24 h of irradiance.

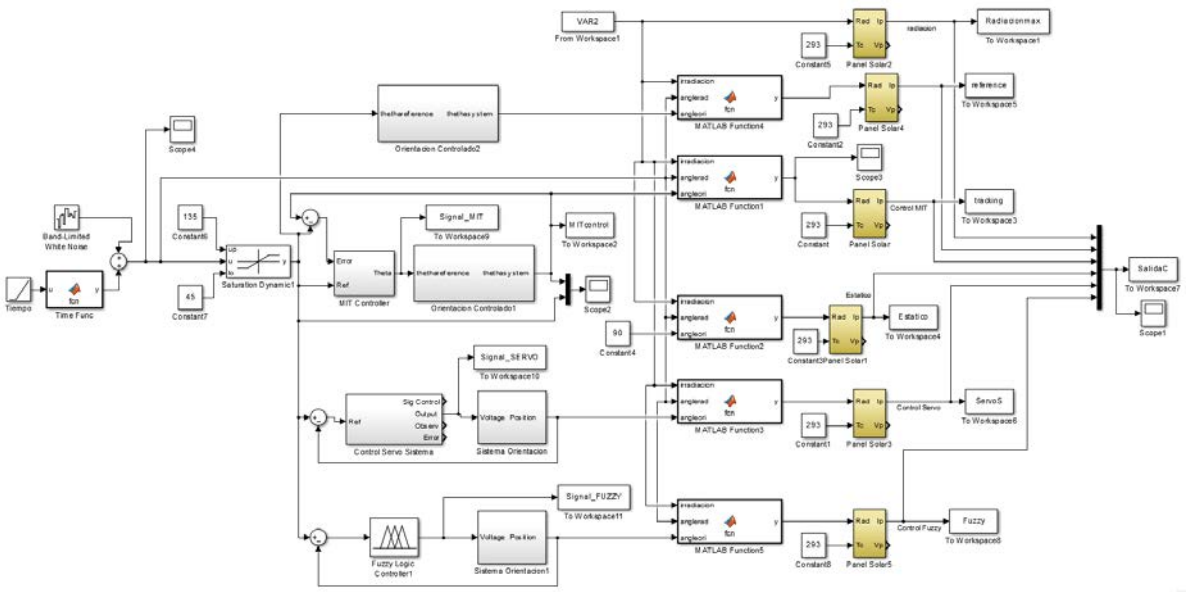

Fig. 9: Simulation block diagram implemented in Simulink®

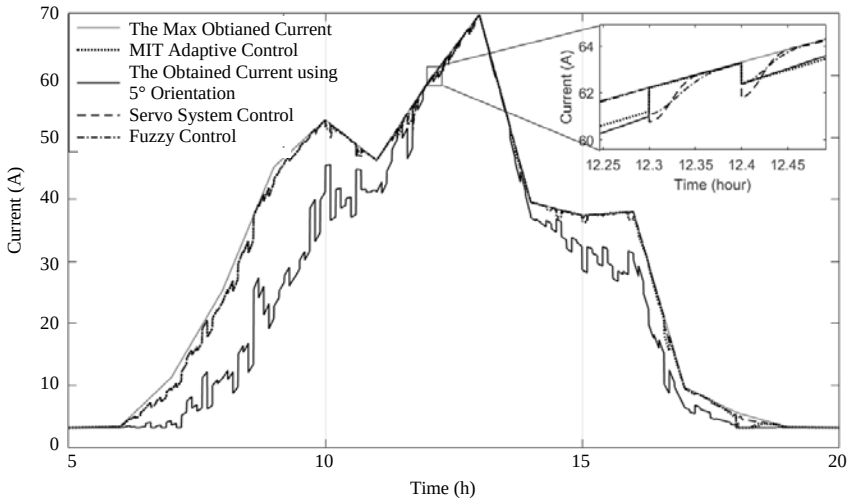

Fig. 10: Currents obtained with controllers simulations

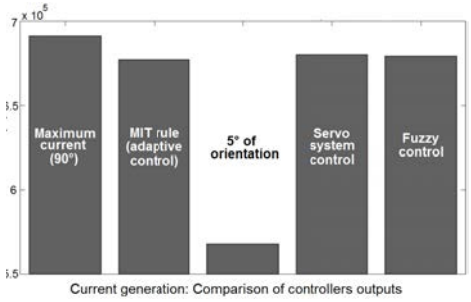

Fig. 11: Bar comparative chart of total current obtained from the PV module with each controller considered during simulation

CONCLUSION

According with the results obtained by the solar tracking system controllers, it is possible to determine that servo system controller is the best controller because is able to adjust its behavior to the changes generated in this system in order to raise the radiation values and also have a larger amount of energy in an efficient way.

Taking into account the MIT rule and fuzzy controllers, we can observe that it have a good behavior due to larger amount of current that, we would obtain applying this controllers into the tracking system. This

controllers are easier to be implemented because it do not have a highest computing architecture and cost in regard to servo system controllers and this is a big advantage.

Considering the solar tracking implementation, it is possible to determine that it is an efficient solution because it always follow the maximum solar radiation that can be generated by the photovoltaic module in regard to static systems as 5° of orientation mechanism because it do not have a continuous tracking with the possibility to acquire the maximum amount of energy always in order to use in an efficient way the nature resources that, we are working with.

If the development is developed in a DC microgrid there would have better efficiency because it improve at 16% of the extra current in a random day (Fig. 11). In a specific application it would help to save most of the energy consumed by traditional loads.

ACKNOWLEDGEMENTS

This research was nancially supported by Nueva Granada Military University, through the project ING-1577 titled "Development, automation and control of a hybrid renewable resources plant" (2014-2015).

REFERENCES

Ackermann, J. and V. Utkin, 1998. Sliding mode control design based on Ackermann's formula. IEEE. Trans. Autom. Control, 43: 234-237.

Anonymous, 2014a. Renewables 2014 blobal status report. REN 21 Steering Committee, Paris, France.

Anonymous, 2014b. Special Report on Climate Change and Land (SRCCL). IPPC, Canada. http://www.ipcc.ch/

Dobakhshari, A.S., S. Azizi and A.M. Ranjbar, 2011. Control of microgrids: Aspects and prospects. Proceedings of the 2011 IEEE International Conference on Networking, Sensing and Control (ICNSC'11), April 11-13, 2011, IEEE, Delft, Netherlands, ISBN: 978-1-4244-9570-2, pp: 38-43.

Edenhofer, O., R. Pichs-Madruga, Y. Sokona, K. Seyboth and P. Matschoss et al., 2011. IPCC special report on renewable energy sources and climate change mitigation. MSc Thesis, Cambridge University Press, Cambridge, UK.

Juang, J.N. and R. Radharamanan, 2014. Design of a solar tracking system for renewable energy. Proceedings of the 2014 Zone 1 Conference on American Society for Engineering Education (ASEE Zone 1), April 3-5, 2014, IEEE, Bridgeport, Connecticut, ISBN:978-1-4799-5232-8, pp: 1-8.

Kar, I. and P.S. Majhi, 2012. Digital control systems: National Programme on Technology Enhanced Learning (NPTEL)-Phase II 781039. Indian Institute of Technology Guwahati, Assam, India. http://nptel.ac.in/courses/108103008/1

Landau, I.D., 1974. A survey of model reference adaptive techniques-theory and applications. Autom., 10: 353-379.

Liu, F.R., X. Li and W.J. Li, 2011. The design of automatic tracking system for solar cell. Proceedings of the 2011 2nd International Conference on Artificial Intelligence, Management Science and Electronic Commerce (AIMSEC), August 8-10, 2011, IEEE, Dengleng, China, ISBN: 978-1-4577-0535-9, pp: 4451-4454.

Mauledoux, M., E. Mejia-Ruda, A. Valencia, O. Caldas and O. Aviles *et al*., 2016. Fuzzy control for solar photovoltaic tracking system. Intl. J. Electr. Energy, 4: 133-136.

Sastry, S. and M. Bodson, 1989. Adaptive Control: Stability, Convergence, and Robustness. Prentice Hall, Upper Saddle River, New Jersey, ISBN:9780130043672, Pages: 377.

Shah, K., P. Chen, A. Schwab, K. Shenai and S. Gouin-Davis *et al*., 2012. Smart efficient solar DC micro-grid. Proceedings of the Conference on Energytech, May 29-31, 2012, IEEE, Cleveland, Ohio, USA., ISBN:978-1-4673-1836-5, pp: 1-5.

Uchida, K., T. Senjyu, N. Urasaki and A. Yona, 2009. Installation effect by solar heater system using solar radiation forecasting. Proceedings of the 2009 Conference on Transmission and Distribution Exposition: Asia and Pacific, October 26-30, 2009, IEEE, Seoul, South Korea, ISBN: 978-1-4244-5230-9, pp: 1-4.